Civil Engineering Infrastructures Journal xx,xx
DOI: 10.22059/CEIJ.2023.348240.1866

Compressive Strength and Microstructural Properties of Sustainable Concrete Containing Nanosilica, Alccofine and Metakaolin

Aabid Hussain Bhat[a,*]

[a]Department of Civil Engineering, National Institute of Technology, Srinagar, India.

[*]Corresponding Authors. Tel. +918491967471

E-mail address: aabid_15phd2017@nitsri.ac.in

Received: 05/09/2022
Revised: 18/01/2023
Accepted: 27/02/2023

Abstract

Structural characteristics of concrete incorporating colloidal Nanosilica (CNS), Metakaolin (MK) and Alccofine (AF) were comparatively studied using X-Ray Diffraction (XRD), Thermogravimetric analysis (TGA), Field Emission Scanning Electron Microscope (FESEM), and Fourier transform infrared spectroscopy (FTIR). The plasticizer demand and compressive strength at 3,7,28 and 90 days of curing ages were also determined. The results indicate that the demand for plasticizer content increased with CNS and MK incorporation owing to their large surface area and rough surface texture respectively. However, AF decreased the plasticizer demand due to glassy surface morphology. Also, the compressive strength increased with replacement ratio. The tetranary blended systems (M6) proved to be more advantageous compared to binary, ternary and normal OPC systems. FTIR, TGA, XRD and FESEM analysis were consistent with the results of compressive strength. The improvement in properties of concrete at early ages is attributed to filler and nucleation effect of CNS and AF. At later ages, CNS modified the CSH by increasing the length of silicate chains, AF and MK diminishes the portlandite content by utilizing it in pozzolanic reaction and filling of pores partially or completely especially by secondary CSH gel, lead to denser structure.

Keywords: Sustainable concrete, Compressive strength, SEM, XRD, TGA/DSC, FTIR

Statements and Declarations:

Acknowledgments
This study was financially supported by Ministry of Human Resource Development, India, in the form of monthly scholarship and the authors are grateful for that. Also, we appreciate and are thankful to the technical staff of laboratory facilities of National Institute of Technology, Srinagar.

Conflict of Interest: There is no conflict of interest.
Funding: This research is supported and funded by the Ministry of Human Resource Development India, through monthly stipend.

Data availability: This paper contains all of the data generated or analysed during this investigation.

1. Introduction

The quest for developing green concrete is increasing considerably during the present times as the demand from construction industry and environmental protection agencies increased. Considerable research has been carried out to study the use of mineral admixtures or supplementary cementing materials (SCM) as partial replacement to cement. These mineral admixtures are either produced from natural sources (Kaolinite, limestone etc) or are by-products or waste materials (Fly ash, silica fume, Slag, etc) from different industries. The engineering benefits by using these admixtures mainly resulted from their fine particle size and pozzolanic reactivity (Malhotra and Mehta, 2004).

Pozzolanic materials mainly silica fume, flyash, rice husk ash, slag etc have been used extensively in construction industry. The improvement in concrete properties due to the addition of slag as cement replacement has increased significantly and various specifications have been laid for manufacturing and use of slag cement in concrete mixtures (Bureau of Indian Standards, 2015). The mechanism responsible for improvement is well documented (Özbay et al., 2016). The properties and microstructure development are critical to figure out the long-term performance typically in marine and acidic environmental conditions. The slow microstructure development at the early ages provides less resistance to adverse effects of surrounding environment. Alccofine (AF) or ultrafine slag is a new generation SCM having superior properties compared to normal slag, especially the strength gain at early ages. It is produced through a controlled granulation process resulting in an ultra-fine particle size and high reactivity. Compared to the normal slag, AF has produced concrete with better performance especially in terms of workability, segregation resistance, improvement in

strength development and durability characteristics, owing to their large specific surface area of particles (Kavyateja et al., 2019; Shaat et al., 2020). Sharmila and Dhinakaran, (2015)studied the effect of replacement of cement by 0 – 15% AF and reported that 10% AF produced concrete with superior hardened properties.

The metakaolin (MK) as SCM on the other hand has received considerable interest from researchers due to its higher pozzolanic characteristics (Abdelli et al., 2017; El-Diadamony et al., 2018). MK is produced from calcination of kaolin clay at 650-800℃(Medri et al., 2020), substantially lower energy requirement for production compared to clinker (1400℃). This means that the production energy and cost of MK are comparatively less than cement. Besides this, the difference with other SCMs is the MK is primary product and others are secondary or by-products. Therefore, MK can be manufactured in a controlled process with desired characteristics. Wild et al., (1996) stated that MK is far superior than other pozzolans as it has the ability to accelerate the cement hydration, and specified that MK seems playing a catalytic effect on hydration reaction.

Various researchers have reported that MK increased the strength parameters at later ages (Ashok et al., 2021; Lima et al., 2023). Some studies even reported the increase of strength at early ages also. The increase in strength at early age is believed to be as a result of pore filling effect of fine MK particles which occupy the space left between the cement grains (da Silva Andrade et al., 2018). However, the strength gain at later ages is as a result of pozzolanic reaction of MK with portlandite, which increases the hydrated aluminium silicates responsible for strength gain and improvement in durability properties like resistance to water and chloride ingress, sulphate and acid resistance etc (Abdelmelek and Lubloy, 2021; Bhat and Naqash, 2022; F. Wang et al., 2018). Although some studies have reported(Al et al., 2018; Sujjavanich et al., 2017; Zhan et al., 2020) the effects of introducing metakaolin as cement replacements however a systematic behaviour of MK was lacking.

Besides these continued efforts of replacing cement with mineral admixtures, various researchers (Hamed et al., 2019; Senff et al., 2012) anticipated that the quick advancement of nanotechnology might be effective for pushing concrete technology to next level in order to meet the desired qualities of concrete and its sustainability goals. For this, some studies (Rong et al., 2020; X. F. Wang et al., 2018) have reported the impact of nano silica on performance of concrete and observed a considerable increase in strength and transport properties compared to normal concrete. The improvement of concrete performance is attributed to the filling effect and pozzolanic properties. However, it is also stated that due to its small size and high specific surface area, it has enhanced the rate of cement hydration by acting as nucleating agent. Uddin et al., (2015) has studied the effect of nanosilica with silica fume and flyash in blended cement composites, and observed that strength, durability and microstructure were enhanced.

1.1 Research Significance

The focus here was to develop a sustainable concrete matrix with enhanced characteristics than conventional concrete. This work studied the effect of replacing cement partially by AF, MK and CNS. Although the influence of binary additives on properties of concrete have been studied. However, hardly any study is available in which the combined effect of CNS, MK and AF have been thoroughly studied. Therefore, this has been the motivation behind this study and it is highly reckoned that this will be useful for various stakeholders intending the usage of CNS, MK and AF in cement composites. This research studied binary, ternary and quaternary blended concrete composites of CNS, MK, AF and Portland cement. The effect of CNS (0-0.45%), MK (0-20%) and AF (0-20%) on workability and compressive strength were studied. Microstructural characterisation was carried out using various analytical tools such as X-Ray Diffraction (XRD), Thermogravimetric analysis (TGA), Field Emission Scanning Electron Microscope (FESEM), and Fourier transform infrared spectroscopy (FTIR) for supporting the experimental results.

2. Materials and methods

2.1 Materials

The various materials used during this experimental work:

- Cement (OPC grade 43), confirming to BIS: 8112 (2013) and ASTM type-I, supplied by Khyber Industries Pvt. Ltd.
- Nanosilica in colloidal form (30.58% solid content), manufactured and supplied by BEE CHEMS.
- AF, commercially manufactured and supplied by Counto Microfine Products Pvt. Ltd.
- MK was supplied by Kaomin Industries LLP.
- Good quality and well graded coarse aggregates of crushed boulders with maximum size of 20mm and well graded river sand of maximum size of 4.75 mm were used during this experimental work. The specific gravity of coarse and fine aggregates determined experimentally were of 2.79 and 2.6 respectively. The gradation curves have been plotted and presented in Fig. 1.
- Auramix-400, a poly-carboxylate ether-based plasticizer, was used as water reducing admixture, supplied by Fosroc Constructive Solutions.

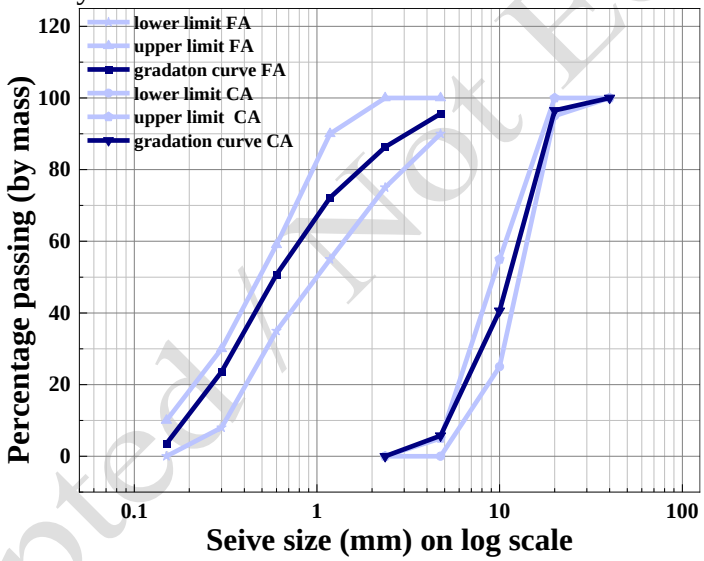

Fig. 1 Particle size distribution of aggregates

Table 1 shows the composition of Cement, CNS, MK and AF and Table 2 shows the characteristics and properties of cement used during this experimental work. From Table 2, it can be observed that CNS contains 99.5% silica, AF contains 35.5% of silica and 21.20% of alumina and MK contains 52.52% of silica and 44.74% of alumina. The particle shape of MK, Cement and AF were observed under FE-SEM and are presented in Fig. 2. XRD analysis was carried out on MK, AF, Cement and CNS to identify the crystalline phases Fig. 3.

Table 1. Physical and chemical characteristics of Cement, MK, AF and CNS

Chemical charcteristics	Cement	MK	AF	CNS
SiO_2 %	19.44	52.54	35.51	99.55
Al_2O_3 %	4.73	44.72	21.21	<0.003
Fe_2O_3 %	3.14	0.4	-	<0.001
CaO %	62.3	0.14	32.3	-
MgO %	3.00	0.17	6.12	-
SO_3 %	3.48	0.00	0.11	-
Loss on ignition %	2.16	0.48	0.68	-

Physical characteristics				
Form	Powder	Powder	Powder	Colloidal
Colour	Greyish	Pinkish white	Light grey	White
Size	-	0.6-1.41µ	4-6 µ	5-40 nm
Blaine Fineness (m^2/kg)	350	1670	1030	-
Specific gravity	3.14	2.61	2.87	1.22

Table 2. Properties and characteristics of Cement

Specific gravity	**Consistency**	**Setting time (min)**		**Compressive strength (MPa)**	
		Initial	Final	7 days	28 days
3.14	29.55%	119	225	35	46

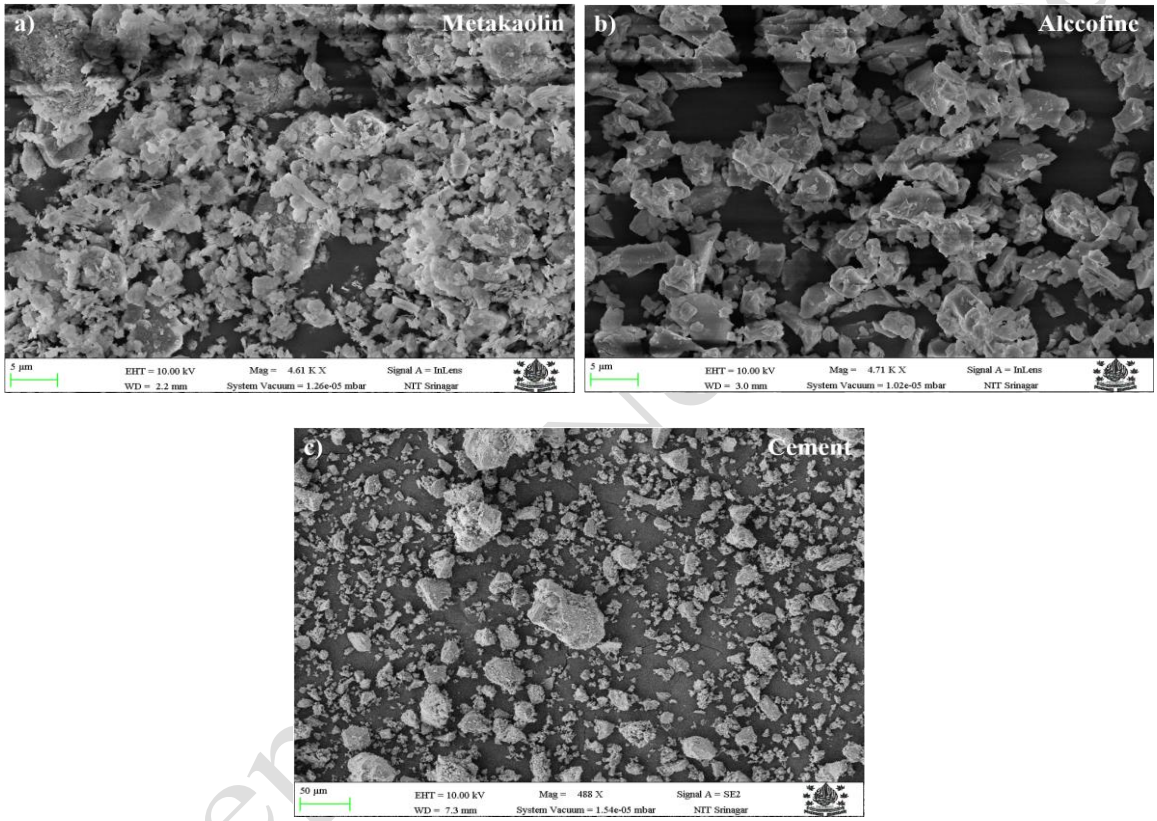

Fig. 2 FESEM of (a) MK (b) AF and (c) Cement

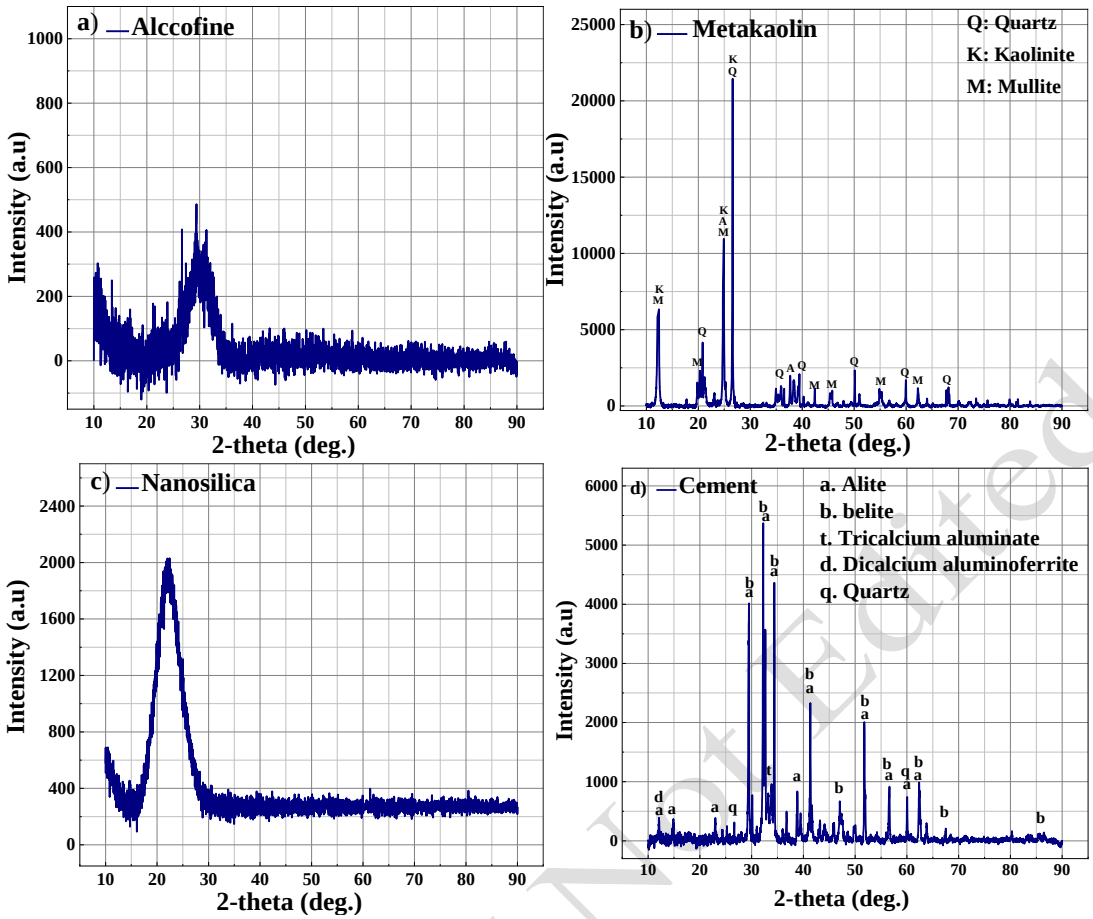

Fig. 3 XRD analysis of (a) AF (b) MK (c) CNS and (d) Cement

2.2 Mix proportions

Trials for preparation of concrete mixtures of target strength 38 MPa for reference mixture at 28 days of curing age were carried out. The water to cement ratio was kept constant at 0.44. Nine different mixtures with varying replacement ratios of MK, AF and CNS were examined to study the influence on strength, workability and microstructural characteristics of concrete mixtures. Table 3 lists the specifics of each of these mixes. The reference mix didn't contain any mineral admixtures. Trials were also conducted for optimum dosages of plasticizer for achieving a target slump around 70 mm. The dosages were carefully selected in order to reduce the adverse effect of overdosing.

Table 3. Mix design

Mix Proportion	MK (%)	AF (%)	CNS (%)	Cement (kg)	MK (kg)	AF (kg)	CNS (kg)	FA (kg)	CA (kg)	Water (kg)	Plasticizer (gm)
M0	0	0	0	350	0	0	0	747	1190	154	1989
M1	0	0	0.45	348.425	0	0	1.575	747	1190	154	2623
M2	0	20	0	280	0	70	0	747	1190	154	1523
M3	20	0	0	280	70	0	0	747	1190	154	3443
M4	0	20	0.45	278.425	0	70	1.575	747	1190	154	1858
M5	5	15	0.45	278.425	17.5	52.5	1.575	747	1190	154	2203
M6	10	10	0.45	278.425	35	35	1.575	747	1190	154	2871
M7	15	05	0.45	278.425	52.5	17.5	1.575	747	1190	154	3557
M8	20	0	0.45	278.425	70	0	1.575	747	1190	154	4247

2.3 Sample preparation

All the concrete mixtures were prepared in a laboratory mixer of 100 litre capacity. Firstly, coarse aggregates, sand, cement, mineral admixtures were fed to a rotary mixer and dry mixed for 2 minutes. Subsequently half of water with CNS was added fallowed by plasticizer and remaining water. The mixing was continued for 5 minutes for obtaining a homogeneous mixture. The concrete batch was removed in a pan and tested for slump. The concrete was then poured into the suitable moulds and compacted with a vibrating table. The surface was finished using a chisel for smooth finish. After 24 hours, all of the specimens were de-moulded and cured in a pool of water (Fig. 4) till the testing age.

Fig. 4 Curing of specimens in curing tank

2.4 Test methods

Compression tests were performed on compression testing machine as per (BIS 516, 1959). The results were analysed statistically using ANOVA (Analysis of variance) and Duncan's homogeneity test with a confidence level of 5%. After completion of compression test at 28 days, the mortar pieces were collected, ground sieved through 45µm sieve and were kept for XRD, TGA/DSC and FTIR analysis. XRD analysis was carried out on powdered concrete specimens by Rigaku Smart Lab Xray diffractometer under the standard conditions of Cu kα=1.54Å. The data was obtained between 5º-60º 2θ with step size of 0.02º and was processed and analysed by using PANalytical X'pert Highscore plus software. FTIR spectroscopy was carried out by using AIM-9000 spectrometer operating in the transmittance range of 4000-400 cm^{-1}. Thermal analysis (TGA/DSC) using Mettler-Toledo TGA/DSC+ GmbH was used to observe the weight loss and decomposition of hydration products particularly the consumption of portlandite with increase in temperature from 0-800℃. For FESEM small concrete chips were removed from the core of cubes and were used for FESEM observations using Zeiss Gemini-500. The specimens were polished, carbon coated and gold plated prior to FESEM analysis.

3. Results and discussion

3.1 Plasticizer demand

The workability of all concrete mixtures was evaluated by using slump test. The slump was kept fixed at around 70 mm and the dosages of super plasticizer (SP) were changed depending on the demand of added SCM's. Fig. 5 shows the usage of plasticizer of all mixtures. As can be seen the demand of SP increased drastically with CNS and MK. However, the AF has increased the Slump and hence less amount of SP was used. The effect of AF on workability

can be attributed to the glassy surface morphology as was observed during FESEM analysis. Owing to this characteristic property, less water was used for surface wetting and therefore more water was available for assisting workability. This was also reported by (Gopinathan and Anand, 2018; Y B et al., 2021). However, the flaky and porous structure of MK (Khan et al., 2020) and the increased surface area of CNS have reduced the free water in matrix. In case of ternary and quaternary mixtures same effects were observed. The maximum and minimum SP demand was shown by M2 (20% MK and 0.45% CNS) and M8 (20% AF) respectively.

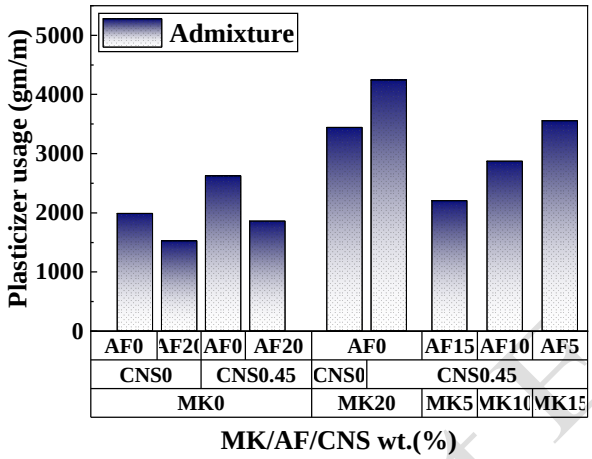

Fig. 5 Plasticizer demand of all concrete mixtures

3.2 Compressive strength

Compressive strength (CS) is said to be one of the main characteristics of concrete quality. Fig. 6 illustrates the CS test results of normal and blended concrete systems containing 0-0.45% CNS, 0-20% AF and 0-20% MK. The results reveal that there is significant strength difference between normal and modified concrete mixtures. The ANOVA test was performed and different mixture combinations were considered as independent variables and CS as dependent variable. The results are displayed in Table 4. Duncan's multiple range test (DMRT), a post hoc test for determination of critical comparison between means, was also performed. The results of DMRT and CS are shown Table 5. It was observed that concrete compositions were significant in CS as the P-value (0.000146) was very less than confidence level (0.05).

Binary concrete mixtures containing 0.45% CNS and 20% AF had CS comparatively higher and very close to normal concrete at 28 days of curing age. However, in Duncan test, these mixtures (M_1 and M_2) were in in the same homogeneous group as that of normal concrete. It was also observed that the early age strength was improved (Abd.el.aleem et al., 2014; Flores et al., 2017; Hou et al., 2013) owing to nucleation (pore filling) and pozzolanic reactions, which reduced porosity and increased density of interfacial transition zone (ITZ), and therefore increased strength development. This behaviour resulted due to formation of more complicated and dense layer of hydrates that covered and firmly bound the fillers together (Salemi and Behfarnia, 2013). The ternary mixture (M4) containing both CNS (0.45%) and AF (20%) had higher CS than binary mixtures and was between groups 2 and 3 in the Duncan's test.

The binary mixture M3 and ternary mixture M8 had CS less than the normal concrete with M3 in group 1 and M8 in between groups 1 and 2. The quaternary mixtures had highest strength values, with M7 between groups 3 and 4, M5 and M6 in group 4. In M6 mixture, there was an increase in CS of 41.81% compared to normal concrete mixture. The strength difference between M6 and M3 was 53.17 %, whereas the strength difference between M3 and normal concrete mixture was -7.42 %. Similarly, the strength difference between M6 and M4 was 22.26 %, while the strength difference between M4 and normal concrete was 15.98 %. As a result of the above investigation, it is possible to conclude that the included SCM's have a synergistic impact, as was also reported by (Bhat and Naqash, 2022; Sousa and Rêgo, 2021).

The increase in strength in modified concrete mixes can be attributed to addition of CNS in system which not only behaves as filler but also acted as activator for pozzolanic reaction of MK and AF, and thereby densifying the microstructure and increased the strength development.

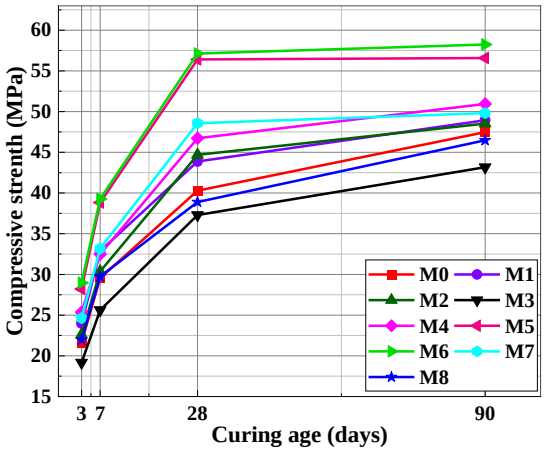

Fig. 6 Compressive strength of concrete with and without MK, AF and CNS

Table 4. Test results of ANOVA at 28 days

Response variable	Input variable	Sum of squares	Mean sum of squares	F- value	p-value	Significance
CS	Mixture composition	1213.04	151.63	7.9	0.000146	Yes

Table 5. CS and Duncan homogeneous groups at 28 days

Mixture	Compressive strength (MPa)	Standard deviation (MPa)	Groups			
			1	2	3	4
M3	37.29	5.92	X			
M8	38.89	3.96	X	X		
M0	40.28	5.18	X	X	X	
M1	43.87	4.93	X	X	X	
M2	44.68	2.07	X	X	X	
M4	46.72	5.63		X	X	
M7	48.57	5.68			X	X
M5	56.4	0.81				X
M6	57.12	1.28				X

3.3 Microstructural characterisation

3.3.1 X-Ray Diffraction

XRD patterns of M0, M1, M2, M3, M5 and M6 concrete mixes at 7 and 28 days of curing age are presented in Fig. 7 and 8. The patterns of normal concrete indicates that Dicalcium and tricalcium silicates were observed and were still present inside the matrix at 28 days of age. However, the intensity of their peaks was less at 28 days compared to intensities at 7 days. The peaks of gypsum were not observed at 7 and 28 days of testing; which is evidence of tricalcium aluminate hydration during early days (Black et al., 2006). The peaks corresponding to the portlandite phase increased with curing age which was obvious owing to hydration of silicates of clinker releasing CSH and portlandite. At 28 days of testing, peak intensity of calcium

sulfoaluminate (ettringite) decreased which may be due to its transformation into a more stable calcium aluminate hydrate form, also reported by (Barbhuiya et al., 2015). The quartz phase present with the aggregates were also present (Bhat and Naqash, 2022). Carbonates were also detected and their intensity increased with age. The carbonates are mainly formed due to the reaction of atmospheric carbon dioxide with hydration products (Liu et al., 2019).

XRD patterns of binary mixtures M1, M2, and M3 containing CNS, MK and AF respectively as shown in Fig. 7 indicate that dicalcium, tricalcium silicate and portlandite peaks were also present however their peak intensities were less than normal concrete. The additional peak of Hydrotalcite was observed in mixture containing AF (Blotevogel et al., 2020). The decrease in peaks corresponding to silicates of clinker were credited to the dilution effect of MK and AF and also the CNS increased the hydration rate by increasing the nucleation site for hydration reaction. The decrease of portlandite peak indicates its consumption in pozzolanic reaction.

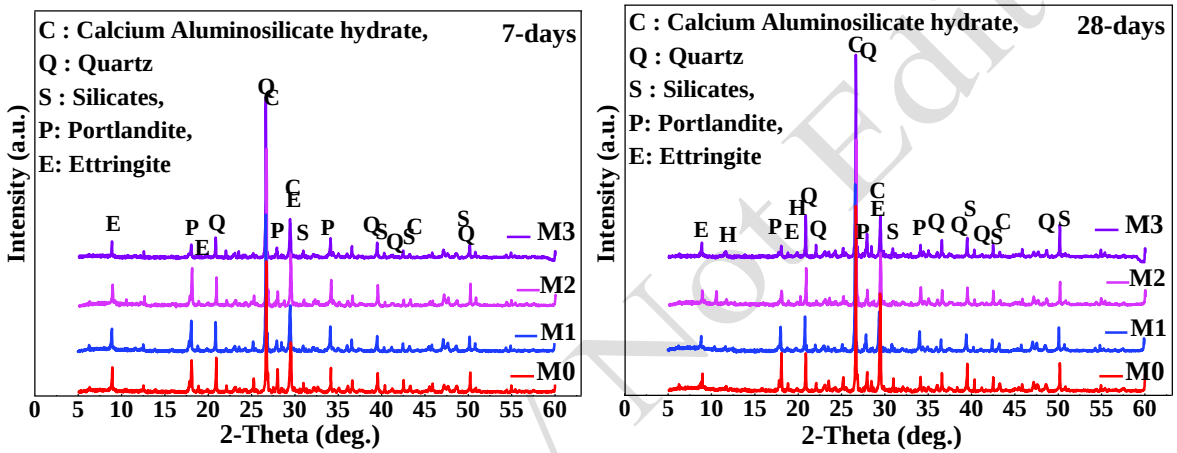

Fig. 7 XRD patterns of M_0, M_1, M_2 and M_3 at 7 and 28 days

Fig. 8 shows XRD patterns of tetranary concrete mixtures (M5 and M6) containing Cement, CNS, MK and AF at 7 and 28 days of curing. The patterns illustrate that the peak intensity of portlandite was less than binary and normal concrete due to pozzolanic reactions of CNS, MK and AF with portlandite. Also, the peaks corresponding to carbonates and un-hydrated silicates decreased with hydration; indicating less carbonation of concrete with CNS, MK and AF. The quartz and cristobalite phases of fine aggregates were also observed. The formation of Hydrotalcite phase was observed; However, the peak intensity was less than binary mixture containing AF only SCM.

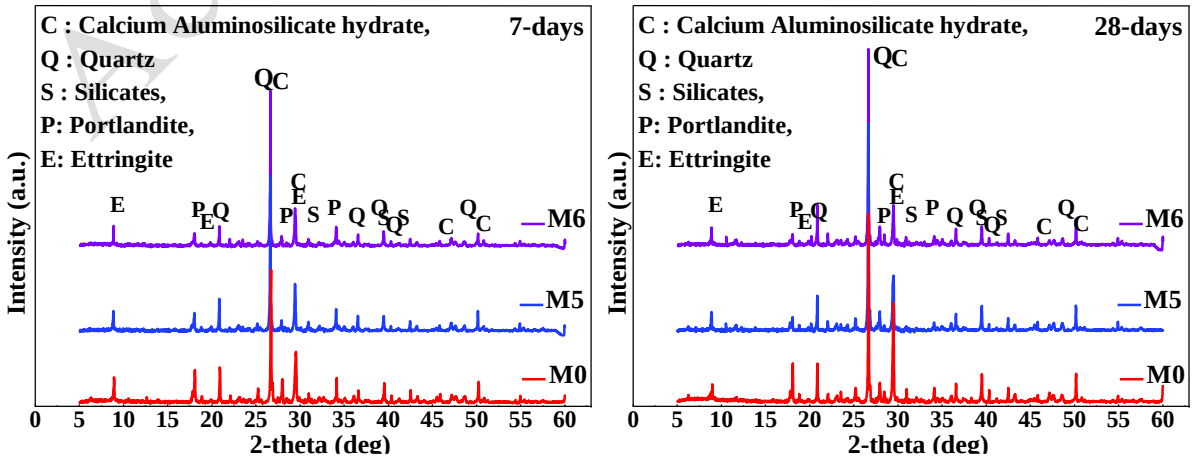

Fig. 8 XRD patterns of M_6 at 7 and 28 days

3.3.2 TG/DSC analysis

TG analysis has been used to determine the quantity of portlandite content in all mixtures and Fig. 9 (a) and (b) shows the TG obtained TG and DTG curves respectively. From DTG curves, the peaks between the temperature range of 25-300℃ are due to elimination of free water, dehydration of hydrates etc. Decomposition of portlandite in all mixtures was observed in the temperature range of 395-530℃ and the corresponding weight loss at this temperature was calculated from TG curves. By using stoichiometry, the total content of portlandite decomposed in all mixtures was calculated and shown in Table 6. The portlandite index was calculated as the ratio between portlandite content of every mixture and normal concrete mix. Moreover, the peaks between 580-790℃ are from the decomposition of carbonates and the mass loss during this temperature range was significant (Reddy and Naqash, 2019).

From results obtained (Table 6), it can be seen that, portlandite content decreased with the incorporation of SCM's in all concrete mixtures compared to reference mix and the maximum decrease was shown in M6. It was also observed that AF in M4 lead to decrease in portlandite more than MK in M3.

Table 6. Quantification of portlandite from TG analysis

Mixture	Portlandite g/100g of paste	Portlandite Index
M0	18.67	1
M1	17.23	0.922871
M2	13.94	0.746652
M3	14.27	0.764328
M5	11.35	0.607927
M6	10.08	0.539904

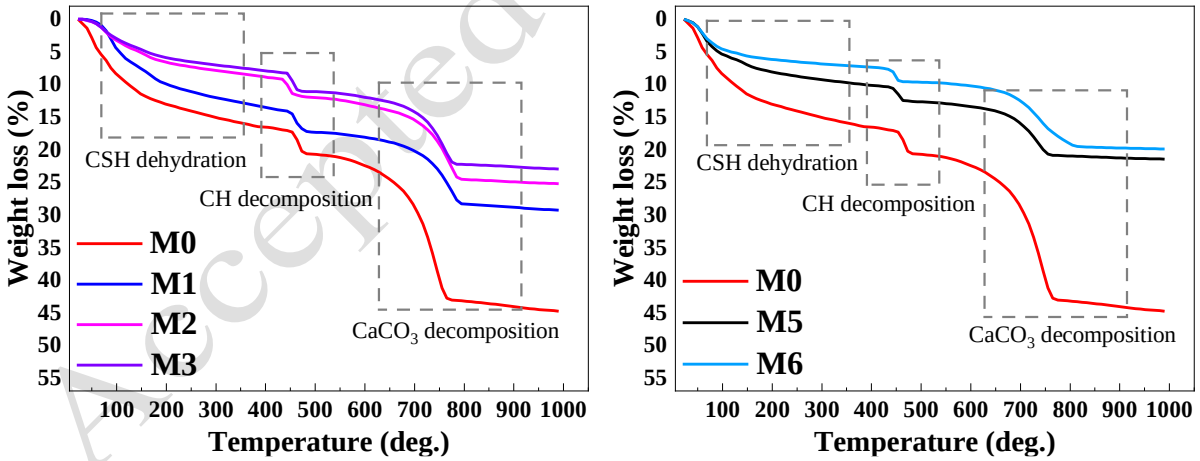

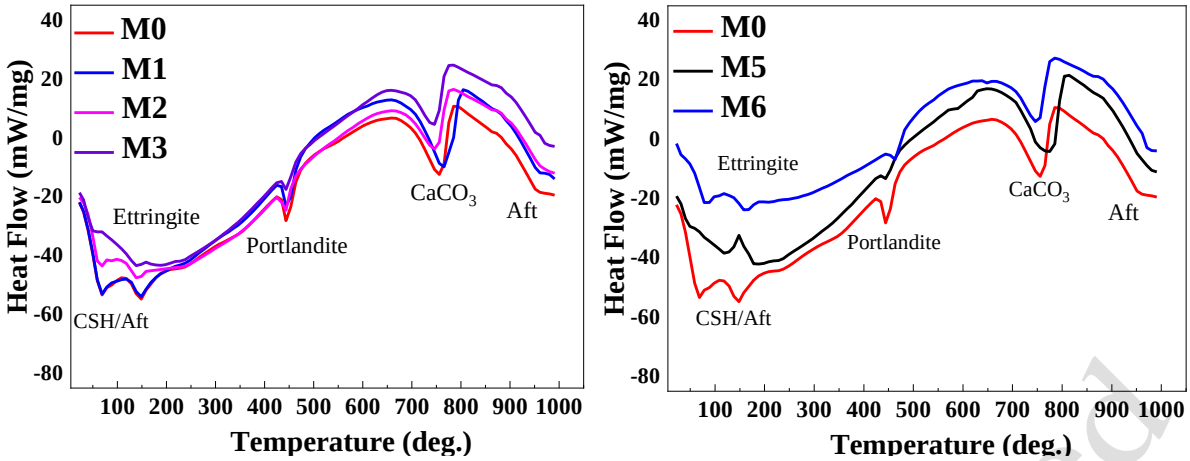

Fig. 9 TG and DSC curves of all mixtures at 90 days

3.3.3 FTIR analysis

Infrared spectrum of all concrete mixtures obtained by FTIR spectroscopy are presented in Fig. 10. The band observed in all mixtures at 3637-3643cm^{-1} are associated to the functional O-H bonds of portlandite and the asymmetric stretching Si-O-Si bonds of CSH (Tobermorite) are observed at 975-959 cm^{-1} and these are consistent with the study (Abd.el.aleem et al., 2014). Comparing the mixtures, it is observed that normal concrete mixture has lowest transmittance at portlandite band and M6 has the highest transmittance value which indicates the lowest portlandite content (Ma Guerrero Bustos et al., 2014; Ping et al., 1999). These observations can be attributed to the pozzolanic reactions of incorporated SCM's. Moreover, in case of CSH band, the highest transmittance was observed in normal concrete and lowest in case of M6 mixture which indicates the possibility of higher CASH content compared to normal concrete. The bands at 1638-1647 cm^{-1} are of chemically bound water (H-O-H) of calcium silicate hydrates (Abd.el.aleem et al., 2014). Stretching vibrations of S-O (SO_4^{2-}) at 1068-1084 cm^{-1} are the characteristic peaks of ettringite mono-sulfo-aluminate presence in mixtures. The intensity of which decreased with hydration and addition of SCM's. Also, the strong bending and stretching vibrations of C-O bonds at 875-861cm^{-1} and 1393-1416cm^{-1} are of carbonates present, possibly coming with the aggregates or the absorption of atmospheric carbon dioxide during hydration.

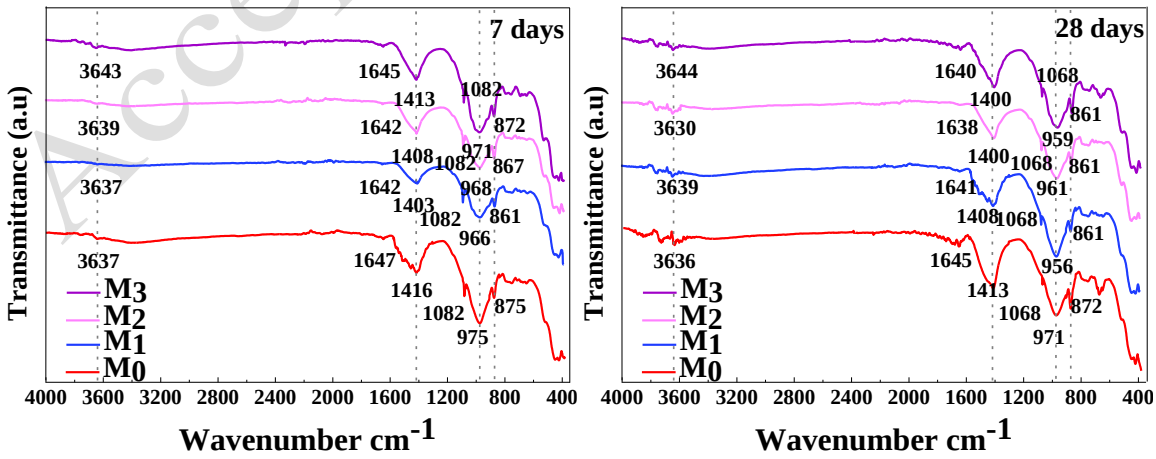

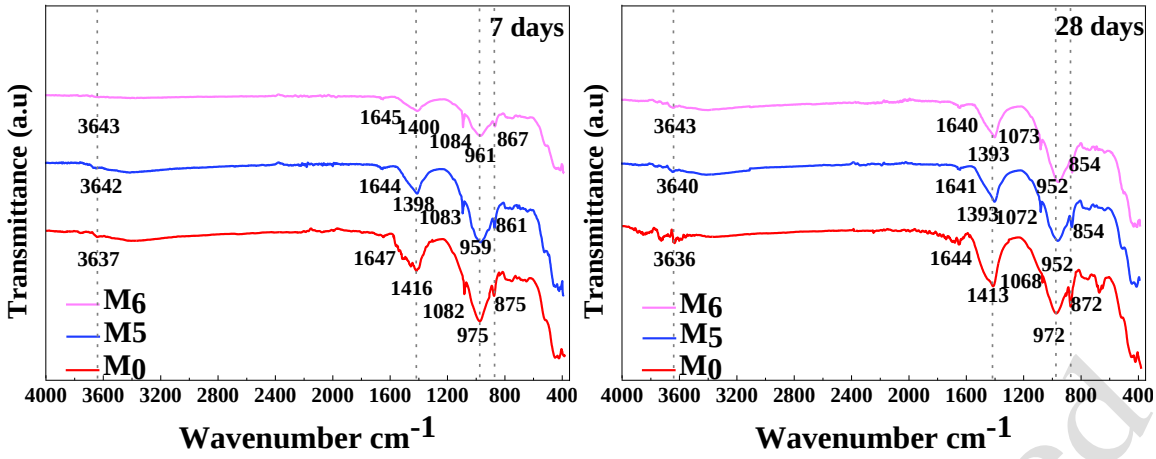

Fig. 10 FTIR spectrum of hardened concrete at 7 and 28 days

3.3.4 FESEM

The microstructure of concrete specimens M_1, M_2, M_3, M_4 and M_6 were examined by FESEM and the effect at 28 days of curing age on ITZ morphology is presented in Fig. 11. Specimens were taken out from the centre of concrete specimens. Fig. 11(a) shows the micrograph of M1 concrete specimen. It illustrates the porous structure and also the hydrated products like CSH gel, Portlandite crystals are clearly noticeable. Between the hydration compounds and other solids, pores of variable sizes are clearly recognized. In contrast, the microstructure of M1, M2 and M3 (Fig. 11 (b-d)) are less porous, homogeneous and more uniform than M1. Therefore, it was expected that the compressive strength could be improved due to improved ITZ. Fig. 11 (e and f) shows microstructure of M5 and M6 and it can be seen that the ITZ is more uniform, and compact compared to binary mixtures; which proves the synergistic properties of CNS, MK and AF.

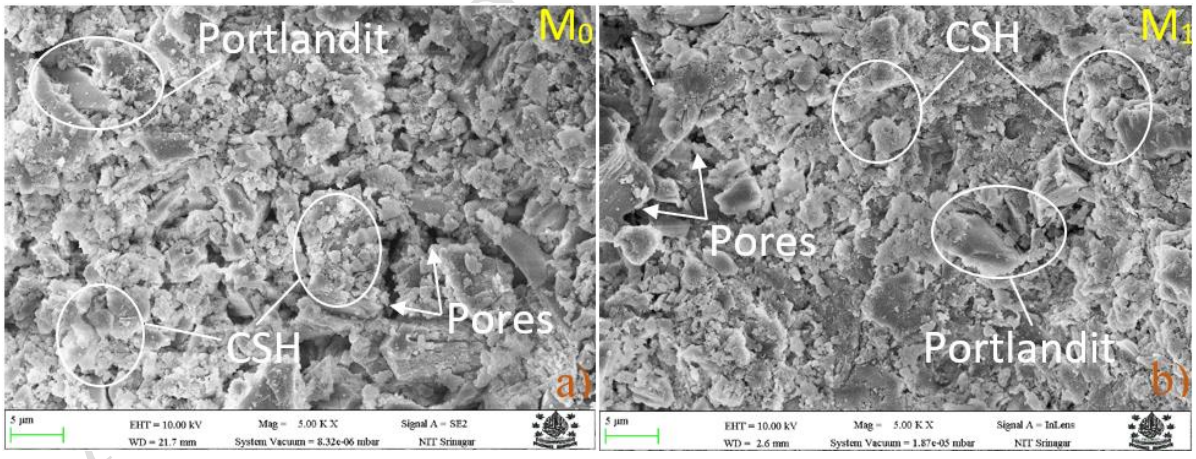

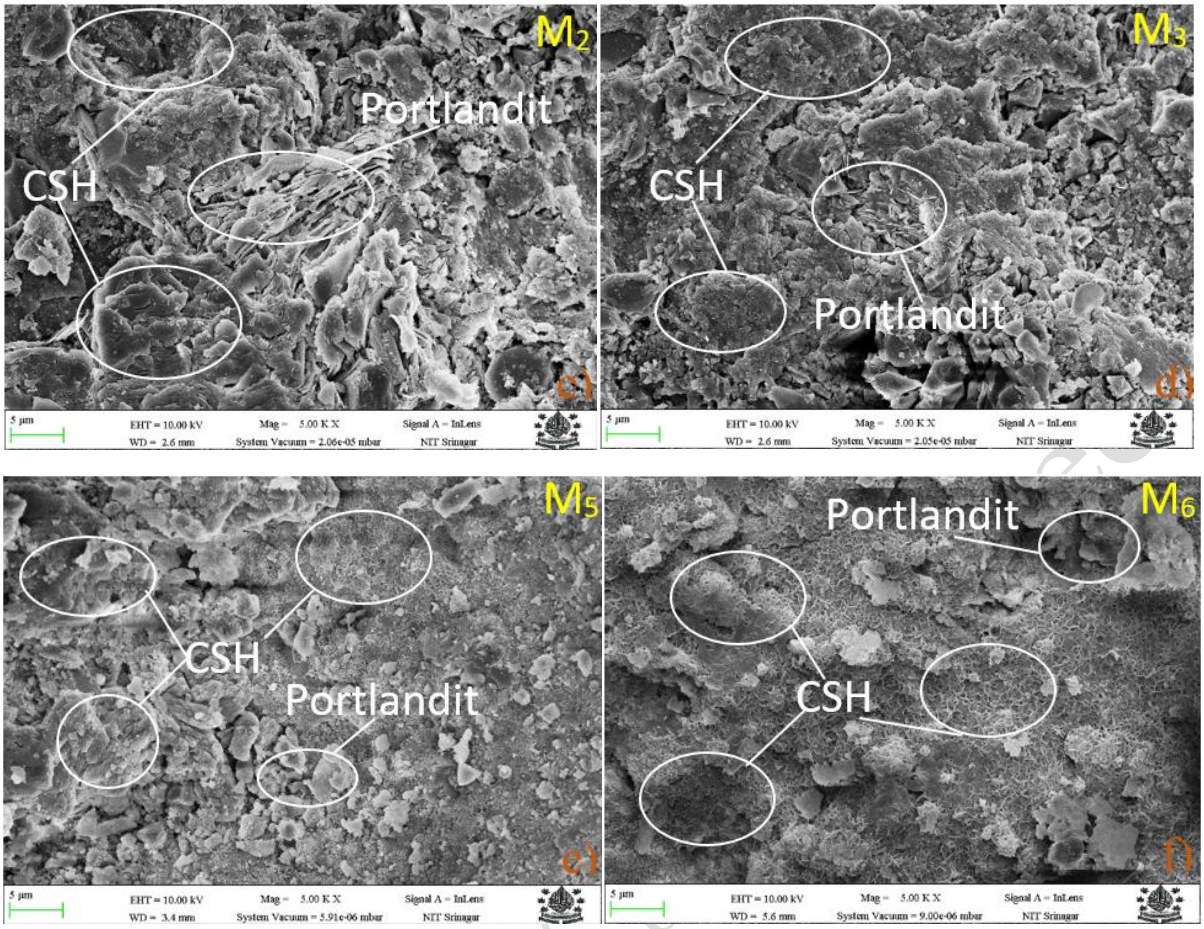

Fig. 11 FESEM images of hardened concrete microstructure at 28 days

3.4 Synergistic approach of CNS, MK and AF

The CNS, MK and AF combination could improve the strength and microstructure as follows: the incorporation of small amount of CNS particles will accelerate and promote the cement hydration by providing additional sites. The hydration products will deposit on these nano sized particles and start growing to form conglomerates in which the CNS particle acts as nucleus. By this, the uniformly dispersion of nanoparticles will enhance microstructure by uniformly distributing conglomerates between the aggregates. Besides this, silica nanoparticles will also prevent the growth of portlandite, Afm and Aft crystals; which are unfavourable for the strength of concrete. Also, the nanoparticles will fill the pores and therefore disrupts pore structure of concrete, which will reduce transport characteristics of concrete. However, in case of higher CNS content, the segregation of CNS particles creates weak zones and therefore reduce the strength. while as, incorporation of MK and AF participate in pozzolanic reactions with the portlandite and increase the CSH gel content in matrix, therefore the strength further increase compared to binary mixtures as was observed in compression test.

4. Conclusion

For CNS-MK-AF-Cement systems containing up to 20% MK and AF and 0-0.45% CNS, the following broad conclusions can be drawn:

- The demand for plasticizer content needed for keeping the consistency of mixtures with and without SCM's constant, increased with CNS and MK incorporation owing to their

large surface area and rough surface texture respectively. However, AF decreased the plasticizer demand owing to glassy surface morphology.

- CNS and AF are complementary to MK: CNS and AF acts as filler and nucleating sites for hydration reaction, thus improves early strength of concrete while MK improves later strength by pozzolanic reaction that refined the pore structure. The tetranary blended systems M_6 proved to be more advantageous compared to binary, ternary and normal OPC system.
- CNS along with AF and MK proved as better system that modifies and presented a denser microstructure. CNS and AF at early ages, acted as filler and also provided the nucleating sites for precipitation of CSH gel, portlandite and other hydration products. At later ages, CNS modified the CSH by increasing the length of silicate chains (Kontoleontos et al., 2012), AF and MK diminishes the portlandite content by utilizing it in pozzolanic reaction and filling of pores partially or completely especially by secondary CSH gel, leading to denser structure.
- XRD analysis results showed reduction of peak intensities of portlandite with age as well as with replacement of CNS, AF and MK, confirming the utilization of portlandite in pozzolanic reaction and formation of secondary CSH gel, corroborating the results of FTIR and TGA/DSC analysis.

References

Abd.el.aleem S, Heikal M, Morsi WM. Hydration characteristic, thermal expansion and microstructure of cement containing nano-silica. Construction and Building Materials 2014;59:151–60. https://doi.org/10.1016/j.conbuildmat.2014.02.039.

Abdelli K, Tahlaiti M, Belarbi R, Nadjib M. ScienceDirect ScienceDirect Influence of the pozzolanic reactivity of the Blast Furnace Slag Assessing the feasibility of using the and metakaolin on heat mortars temperature function for a long-term district heat. Energy Procedia 2017;139:224–9. https://doi.org/10.1016/j.egypro.2017.11.200.

Abdelmelek N, Lubloy E. Evaluation of the mechanical properties of high-strength cement paste at elevated temperatures using metakaolin. Journal of Thermal Analysis and

Calorimetry 2021;145:2891–905. https://doi.org/10.1007/s10973-020-09992-2.

Al A, Wang Yu, Wang Yan, Augusthus-nelson L. Long term durability properties of concrete modified with metakaolin and polymer admixture. Construction and Building Materials 2018;172:41–51. https://doi.org/10.1016/j.conbuildmat.2018.03.215.

Ashok K, Kameswara Rao B, Sarath Chandra Kumar B. Experimental study on metakaolin & nano alumina based concrete. IOP Conference Series: Materials Science and Engineering 2021;1091:012055. https://doi.org/10.1088/1757-899x/1091/1/012055.

Barbhuiya S, Chow PL, Memon S. Microstructure, hydration and nanomechanical properties of concrete containing metakaolin. Construction and Building Materials 2015;95:696–702. https://doi.org/10.1016/j.conbuildmat.2015.07.101.

Bhat AH, Naqash JA. Experimental studies of sustainable concrete modified with colloidal nanosilica and metakaolin. Journal of Building Pathology and Rehabilitation 2022;7:1–17. https://doi.org/10.1007/s41024-021-00157-8.

BIS 516. Method of Tests for Strength of Concrete,Bureau of Indian Standards; New Delhi, India 1959.

Black L, Breen C, Yarwood J, Deng CS, Phipps J, Maitland G. Hydration of tricalcium aluminate (C3A) in the presence and absence of gypsum - Studied by Raman spectroscopy and X-ray diffraction. Journal of Materials Chemistry 2006;16:1263–72. https://doi.org/10.1039/b509904h.

Blotevogel S, Ehrenberg A, Steger L, Doussang L, Kaknics J, Patapy C, et al. Ability of the R3 test to evaluate differences in early age reactivity of 16 industrial ground granulated blast furnace slags (GGBS). Cement and Concrete Research 2020;130:105998. https://doi.org/10.1016/j.cemconres.2020.105998.

Bureau of Indian Standards. Portland Slag Cement - Specification. IS 455. Bureau of Indian Standards, New Delhi, India 2015;34.

El-Diadamony H, Amer AA, Sokkary TM, El-Hoseny S. Hydration and characteristics of metakaolin pozzolanic cement pastes. HBRC Journal 2018;14:150–8. https://doi.org/10.1016/j.hbrcj.2015.05.005.

Flores YC, Cordeiro GC, Toledo Filho RD, Tavares LM. Performance of Portland cement pastes containing nano-silica and different types of silica. Construction and Building Materials 2017;146:524–30. https://doi.org/10.1016/j.conbuildmat.2017.04.069.

Gopinathan S, Anand KB. Properties of cement grout modified with ultra-fine slag. Frontiers of Structural and Civil Engineering 2018;12:58–66. https://doi.org/10.1007/s11709-017-0383-0.

Hamed N, El-feky MS, Kohail M, Nasr EAR. Effect of nano-clay de-agglomeration on mechanical properties of concrete. Construction and Building Materials 2019;205:245–56. https://doi.org/10.1016/j.conbuildmat.2019.02.018.

Hou PK, Kawashima S, Wang KJ, Corr DJ, Qian JS, Shah SP. Effects of colloidal nanosilica on rheological and mechanical properties of fly ash-cement mortar. Cement and Concrete Composites 2013;35:12–22. https://doi.org/10.1016/j.cemconcomp.2012.08.027.

Kavyateja BV, Guru Jawahar J, Sashidhar C. Investigation on ternary blended self compacting concrete using fly ash and alccofine. International Journal of Recent Technology and

Engineering 2019;7:462–6.

Khan SU, Ayub T, Shafiq N. Physical and Mechanical Properties of Concrete with Locally Produced Metakaolin and Micro-silica as Supplementary Cementitious Material. Iranian Journal of Science and Technology - Transactions of Civil Engineering 2020;44:1199–207. https://doi.org/10.1007/s40996-020-00436-3.

Kontoleontos F, Tsakiridis PE, Marinos A, Kaloidas V, Katsioti M. Influence of colloidal nanosilica on ultrafine cement hydration: Physicochemical and microstructural characterization. Construction and Building Materials 2012;35:347–60. https://doi.org/10.1016/j.conbuildmat.2012.04.022.

Lima NBD, Silva D, Vilemen P, Nascimento HCB, Cruz F, Santos TFA, et al. A chemical approach to the adhesion ability of cement-based mortars with metakaolin applied to solid substrates. Journal of Building Engineering 2023;65:105643. https://doi.org/10.1016/j.jobe.2022.105643.

Liu W, Li YQ, Tang LP, Dong ZJ. XRD and 29Si MAS NMR study on carbonated cement paste under accelerated carbonation using different concentration of CO2. Materials Today Communications 2019;19:464–70. https://doi.org/10.1016/j.mtcomm.2019.05.007.

Ma Guerrero Bustos A, Redondo JJG, Quiñones GPÁ, Elizalde SG. Multi-scale analysis of cement pastes with nanosilica addition. Advances in Cement Research 2014;26:271–80. https://doi.org/10.1680/adcr.13.00023.

Malhotra VM, Mehta PK. Pozzolanic and Cementitious Materials. Amsterdam The Netherlands: Gordon and Breach; 2004. https://doi.org/10.1201/9781482296761.

Medri V, Papa E, Lizion J, Landi E. Metakaolin-based geopolymer beads: Production methods and characterization. Journal of Cleaner Production 2020;244:118844. https://doi.org/10.1016/j.jclepro.2019.118844.

Özbay E, Erdemir M, Durmuş HI. Utilization and efficiency of ground granulated blast furnace slag on concrete properties - A review. Construction and Building Materials 2016;105:423–34. https://doi.org/10.1016/j.conbuildmat.2015.12.153.

Ping Y, Kirkpatrick RJ, Brent P, McMillan PF, Cong X. Structure of calcium silicate hydrate (C-S-H): Near-, mid-, and far-infrared spectroscopy. Journal of the American Ceramic Society 1999;82:742–8. https://doi.org/10.1111/j.1151-2916.1999.tb01826.x.

Reddy PN, Naqash JA. Experimental study on TGA, XRD and SEM analysis of concrete with ultra-fine slag. International Journal of Engineering, Transactions B: Applications 2019;32:679–84. https://doi.org/10.5829/ije.2019.32.05b.09.

Rong Z, Zhao M, Wang Y. Effects of modified nano-SiO2 particles on properties of high-performance cement-based composites. Materials 2020;13:1–12. https://doi.org/10.3390/ma13030646.

Salemi N, Behfarnia K. Effect of nano-particles on durability of fiber-reinforced concrete pavement. Construction and Building Materials 2013;48:934–41. https://doi.org/10.1016/j.conbuildmat.2013.07.037.

Senff L, Hotza D, Lucas S, Ferreira VM, Labrincha JA. Effect of nano-SiO 2 and nano-TiO 2 addition on the rheological behavior and the hardened properties of cement mortars. Materials Science & Engineering A 2012;532:354–61. https://doi.org/10.1016/j.msea.2011.10.102.

Shaat M, Fathy A, Wagih A. Correlation between grain boundary evolution and mechanical properties of ultrafine-grained metals. Mechanics of Materials 2020;143. https://doi.org/10.1016/j.mechmat.2020.103321.

Shaikh FUA, Supit SWM. Chloride induced corrosion durability of high volume fly ash concretes containing nano particles. Construction and Building Materials 2015;99:208–25. https://doi.org/10.1016/j.conbuildmat.2015.09.030.

Sharmila P, Dhinakaran G. Strength and durability of ultra fine slag based high strength concrete. Structural Engineering and Mechanics 2015;55:675–86. https://doi.org/10.12989/sem.2015.55.3.675.

da Silva Andrade D, da Silva Rêgo JH, Cesar Morais P, Frías Rojas M. Chemical and mechanical characterization of ternary cement pastes containing metakaolin and nanosilica. Construction and Building Materials 2018;159:18–26. https://doi.org/10.1016/j.conbuildmat.2017.10.123.

Sousa MIC, Rêgo JH da S. Effect of nanosilica/metakaolin ratio on the calcium alumina silicate hydrate (C-A-S-H) formed in ternary cement pastes. Journal of Building Engineering 2021;38:102226. https://doi.org/10.1016/j.jobe.2021.102226.

Sujjavanich S, Suwanvitaya P, Chaysuwan D, Heness G. Synergistic effect of metakaolin and fly ash on properties of concrete. Construction and Building Materials 2017;155:830–7. https://doi.org/10.1016/j.conbuildmat.2017.08.072.

Wang F, Kovler K, Provis JL, Buchwald A, Cyr M, Patapy C, et al. Metakaolin. RILEM State-of-the-Art Reports, vol. 25, Springer Netherlands; 2018, p. 153–79. https://doi.org/10.1007/978-3-319-70606-1_5.

Wang XF, Huang YJ, Wu GY, Fang C, Li DW, Han NX, et al. Effect of nano-SiO 2 on strength , shrinkage and cracking sensitivity of lightweight aggregate concrete 2018;175:115–25. https://doi.org/10.1016/j.conbuildmat.2018.04.113.

Wild S, Khatib JM, Jones A. Relative strength, pozzolanic activity and cement hydration in superplasticised metakaolin concrete. Cement and Concrete Research 1996;26:1537–44. https://doi.org/10.1016/0008-8846(96)00148-2.

Y B R, Y RR, Hossiney N, H T D. Properties of high strength concrete with reduced amount of Portland cement– a case study. Cogent Engineering 2021;8. https://doi.org/10.1080/23311916.2021.1938369.

Zhan P, He Z, Ma Z, Liang C, Zhang X. Utilization of nano-metakaolin in concrete : A review. Journal of Building Engineering 2020;30:101259. https://doi.org/10.1016/j.jobe.2020.101259.